Aerosol and Air Quality Research, 16: 3026–3036, 2016

ISSN: 1680-8584 print / 2071-1409 online
doi: 10.4209/aaqr.2016.08.0347

The Horizontal and Vertical Characteristics of Aeolian Dust from Riverbed

Jin-Yuan Syu[1], Yu-Chih Cheng[1], Yuan-Yi Kao[1], Chi-Sung Liang[1], Yeou-Lih Yan[2], Chane-Yu Lai[3], Chang-Tang Chang[4], Chih-Chieh Chen[5], Chea-Yuan Young[6], Yee-Lin Wu[7], Wen-Yinn Lin[1*]

[1] *Institute of Environmental Engineering and Management, National Taipei University of Technology, Taipei City 10608, Taiwan*
[2] *Department of Safety, Health and Environmental Engineering, National United University, Miaoli 36003, Taiwan*
[3] *Department of Occupational Safety & Health, College of Health Care & Management, Chung Shan Medical University, Taichung City 40201, Taiwan*
[4] *Department of Environmental Engineering, National I-Lan University, I-Lan City 26047, Taiwan*
[5] *Institute of Occupational Medicine and Industrial Hygiene, National Taiwan University, Taipei City 10055, Taiwan*
[6] *Department of Natural Resource, Chinese Culture University, Taipei City 11114, Taiwan*
[7] *Department of Environmental Engineering, National Cheng Kung University, Tainan City 70101, Taiwan*

ABSTRACT

Arid riverbed is an important source of Aeolian dust to influence the atmosphere of nearby village or downtown. In general, Aeolian dust pertains to wind activity in the study of geology, environment and meteorology on particle suspension. This field study set the horizontal/vertical sampling system up in order to investigate the Aeolian dust dimensional distribution properties from the riverbed of the Jhuoshuei River. In addition, the study utilized the unmanned aerial vehicle (UAV) imagery to discriminate the covering condition of riverbed. The results revealed that the percentage of riverbed covering conditions, including bare zone, wetlands, green covering and water covering was about 50.1, 15.7, 16.8 and 17.4%, respectively, on January 5th, 2011. Two Aeolian dust cases from riverbed were measured on November 26th, 2010 and January 15th, 2011. First sampling case was under slower wind speed, and the total particulate matter (PM) concentration in vertical sampling was almost decreased with increasing sampling height, however, the phenomena of second case (faster wind speed) was just on the contrary. Besides, Aeolian dust was distributed in a bimodal or a multimodal curve, and the main peak size was above 10 µm. Mode size of suspension particle diameter was increased as the wind speed increased (14.8 µm/ first case; 21.3 µm/ second case). The total mass concentration ratio of south site to source site (one meter height) was about 1:9 in first case and about 1:3 in second case. Comparing with those two cases, the faster the wind is, the shorter the surface roughness height is (3.08 mm/ first case; 1.07 mm/ second case). Besides, as the wind speed increasing, the friction velocity was also increased (0.33 m s^{-1}/ first case; 0.68 m s^{-1}/ second case). Consequently, this study clued the spatial variability of river dust events, which can further aid the site investigating, forecasting and preventing of dust influences.

Keywords: Aeolian dust; UAV; Horizontal/vertical sampling; Roughness height.

INTRODUCTION

Aeolian dust is a kind of atmospheric mineral particle, including loess, sand and clay, which is suspended by Aeolian processes. These processes of particulate suspension such as raising, transportation, and deposition are important activities of the geomorphic surface (Offer and Goossens, 1995; Delmas *et al.*, 1996; Field *et al.*, 2009; Field *et al.*, 2012). Especially, the finer and dryer particle are easily suspended by wind force in the arid or semi-arid areas (Goossens and Offer, 1997; Hahnenberger and Nicoll, 2014).

Aeolian dust emissions from semi-arid and arid surfaces ensue from two steps of Aeolian process. First, before dust suspension, particulate will be rolling (creep) and bouncing (saltation) when the friction velocity exceeds the threshold wind friction velocity (Bagnold, 1941; Saffman 1965; Greeley *et al.* 1977; Sharratt and Vaddella, 2014). Particularly, dust collides with bigger sand aggregates by inter-particle forces, in the meanwhile, the abrasion and splintering actions between sand and rock bring finer particles (Kok, 2011). Second, due to Bernoulli's principle, dust was directly carried

[*] Corresponding author.
E-mail address: wylin@ntut.edu.tw

by aerodynamic force and lift force (Kok *et al.*, 2012), causing not only horizontal but also relatively vertical dust flux (mg m^{-2} s^{-1}) for a higher given wind speed (Goossens and Offer, 2000). Sand suspension is not only affected by wind, but also influenced by water indirectly, including river flow and raining. It'll change the moisture content and surface structure of sediment (Karanasiou *et al.*, 2014). Moisture content transforms the soil properties, like viscosity, size, unit weight and elements. And, soil crusting is a kind of surface structure change, which is caused by raindrop force impacting onto the bare zone. The raindrop falling down may seal the porous of surface soil forming sedimentation crusts. The friction velocity of crusting surface is faster than loose surface of the bare zone (WMO, 2008; Webb and Strong, 2011).

Significantly, the Aeolian dust emission is not only affected by the weather condition, but also related to bare zone size, covering condition, and influence time. Some researchers used different tools to know the bare zone size and covering condition, even in air quality measuring, such as unmanned aerial vehicles (UAV) and satellite (Bian *et al.*, 2011; Zhao, 2012; Hahnenberger and Nicoll, 2012; Hugenholtz *et al.*, 2012; Shen *et al.*, 2015). The accuracy of display resolution from UAV was great then satellite imagery. UAV is a significant tool to observe the characteristic on the earth's surface due to the high resolution.

In recent years, the objective of research on dust suspension and transportation has grown rapidly. There are three kinds of method to measure the dust emission, including the theoretical derivation, numerical analysis (wind tunnel simulation), and experimental test (sampling and remote sensing) (Furieri *et al.*, 2013; Modaihsh and Mahjoub, 2013; Margielewski *et al.*, 2015; Vijayakumar *et al.*, 2016). Some researchers measured the PM chemical composition, size distribution, or mass/number concentration in ambient air as well as in the source to identify the different PM periods (Liang *et al.*, 2015; Upadhyay *et al.*, 2015). The results indicated that the suspension particle occupies a vital character in the optical, physical, chemical, and biological effects in the atmosphere, such as visibility, solar radiation, and photosynthesis (McGowan *et al.*, 1996; Erell and Tsoar, 1999; Margielewski *et al.*, 2015). In general, pool visibility is essentially assigned to the extinction of visible light by particles (Friedlander, 2000). Several studies reported that the atmospheric visibility is related to PM (Pillai *et al.*, 2002; Pui *et al.*, 2014; Cheng *et al.*, 2015). The higher the particle mass concentration is, the poorer the visibility is (Kim *et al.*, 2001; De *et al.*, 2005; Cheng *et al.*, 2015). At the same time, dust emission also influences the regional air quality and bring about human health problems (Ono, 2006; Goudie, 2009; Rashki *et al.*, 2013; Goudie, 2014), especially, the contaminants along with dust affect human health as its transport to the densely populated town or city. Not only the visibility, ambient air quality, and health problems, but also global climate effects are influenced by Aeolian dust (Bauer and Ganopolski, 2010; Evan *et al.*, 2014; Lancaster, 2015).

Aeolian dust is frequently happening around our living environment, such as the road dust due to the vehicle moving, human activity or the wind blowing (Karanasiou *et al.*, 2014). Besides, some dust comes from gravel processing site, construction site or dry fallow due to wind blowing (Chang, 2006). Moreover, the sandstorm, which comes from Desert or dry Lake, is most comment environment issues in East Asia, Middle East, North America, Australia and North Africa (Chen *et al.*, 2002; Ono, 2006; Reynolds *et al.*, 2006; Rashki *et al.*, 2013; Zhu and Yu, 2014). It is the transnational materials transfer. The composition of the material particle from the long-term transport sand storm was mostly finer than 10 µm (In and Park, 2003; Pye and Tsoar, 2009). Furthermore, some local places were affected by the river dust that comes from the arid riverbed, which affect the nearby towns (Lin and Yeh, 2007; Vickery and Eckardt, 2013).

Thus far, the Aeolian dust from the Jhuoshuei River is always an important emission source in Central Taiwan (Chen *et al.*, 2015). However, the dust emission features from the riverbed was scarcely investigated, especially for suspension particle size distribution and vertical concentration condition. In order to probe the spatial and temporal variability of Aeolian dust. This thesis tried to explore the characteristic of Aeolian dust emission from a semi-arid riverbed of Jhuoshuei River.

METHODS

The purpose of this measurement tried to provide insights into the relationships between source wind condition and Aeolian dust emission. Therefore, in this section, the study zone and the weather condition were introduced first. After that the UAV imagery analysis process was used to investigate the riverbed current situation. Besides, wherever possible, the wind speed, wind direction, particle size distribution and mass concentration of Aeolian dust were measured for all field sampling sites.

Study Zone and Weather

The exploration was conducted on 26th November 2010 (first case) and 15th January 2011 (second case) in Jhuoshuei River, West-Central Taiwan (Fig. 1). It is the longest river in Taiwan, which is covering 186 km in length. The gradient of Jhuoshuei River is 1/46 in average (Li *et al.*, 2013), however, the gradient of the upstream tributary is on a very steep slope (Yang *et al.*, 2011). Therefore, the erosion process of water is extremely strength due to the orogeny in Taiwan (Siame *et al.*, 2010). The stratum of mountain surface is the sediment from the ocean, and it's young and also active in Taiwan. Therefore, sedimentary rock (shale and slate) is the mainly component of the upstream mountain here. If it's affected by erosion, such as rainfall, river flow or anthropogenic activity, sand and mud will flux along with rapid streams and then deposit in the flat area of the river (Li *et al.*, 2013).

Wind force and moisture are two of the most important weather properties in sand suspension (King *et al.*, 2011). Taiwan is located on the tropic of cancer, and its general climate is the tropical marine and also non-arid here, where the day length and temperature are fluctuating. The annual average rainfall is about 2,129 mm (from 1981 to

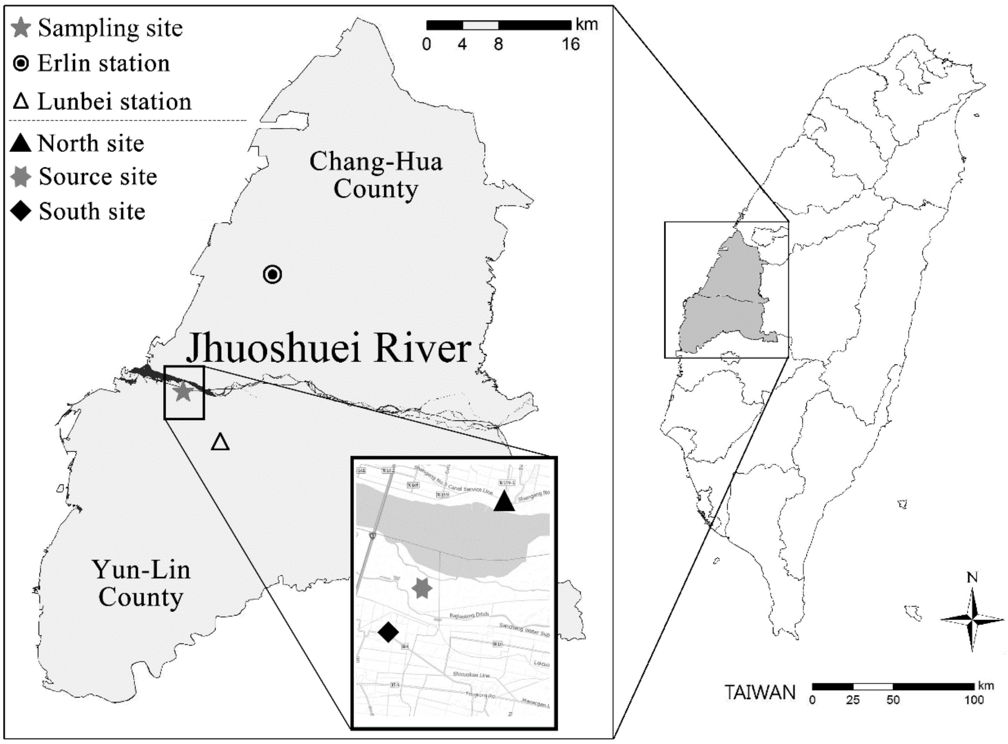

Fig. 1. Map shows the locations of sampling sites in study zone of target arid riverbed. Right part denotes the Jhuoshuei River within the index map of west-central Taiwan.

2015); the rainy season usually happens in summer as the Asian monsoon is coming. In addition, the typhoon is greatest severe weather from June to September (Fang *et al.*, 2009). During the winter and early spring (November–March), central and southern parts of Taiwan are generally sunny and dry. Moreover, the wind energy in Taiwan is copiously due to the Asian northeast monsoon in winter and tropical cyclones (typhoon) in summer. Northeast monsoon is the most important effects of Aeolian dust in Taiwan. Besides, due to the strong sea breezes during the daytime (Pokhrel and Lee, 2011) in winter, the wind speed of monsoon is faster than in summer.

For that reason, this study focused on investigating the effect of Aeolian dust from downstream sandbank of Jhuoshuei River. Thus, the local weather condition (including wind speed and direction) was based on Taiwan EPA air quality monitoring station. As shown in Fig. 1, the background and downstream air quality monitoring station was Er-Lin station in Chang-Hua County and Lun-Bei station in Yun-Lin County, respectively, due to the northeast monsoon. Besides, the sampling not only located on the riverbed (source site) but also measured upon the north embankment (north site) and on the top of a community centre of the nearest south village (south site).

Covering Analysis of Riverbed by UAV Imagery and Computational Chromatic Analysis

In this part, the imagery of the Jhuoshuei River from UAV was analysed in this study that seems to be well suited for providing the covering information. The digital camera (EOS 500D with 50 mm prime lens, Canon) was installed in UAV which used to take the riverbed photograph at 1,200 m height. After that, the computational chromatic analysis was used in river covering and bare zone measurement. However, the original image from UAV was complicated. Thus, before chromatic analysis, the non-river course area was removed by Photoshop CS4. Afterward, the coverings and bare zone were dissected in computational chromatic analysis software "ImageJ". It can calculate area and pixel value statistics of user-defined selections. In brief, the percentage of bare zone, green covering, and water covering areas were calculated by the computational chromatic analysis.

Sampling

Aeolian dust emission is not only horizontal but also vertical transport that spread in three dimensions. Hence, in this thesis, the particulate matter (PM) measurement included horizontal and vertical sampling. The target of horizontal sampling was focused on the relations of the mass concentration increment between north site (upstream), source site (sandbank) and south site (downstream) at sampling site (as shown in Fig. 1). Besides, the vertical sampling, which was five meters height sampling tower, was set-up to collect the Aeolian dust sample from the riverbed at the source site. The PM mass concentration and size distribution were measured by using Marple personal cascade impactor (Model 298, Thermo Andersen Inc., USA) sampler. The aerodynamic diameter range of Marple sampler was from 0.5 µm to 21 µm with a final filter. In principle, the Marple sampler equipped the 34 mm PVC fibres filter. Those filters were conditioned in a conditioning room for 24 hours where the relative humidity (RH) and temperature was kept at 40 ± 5% and 20 ± 1°C, respectively. And then, all sampling filters were weighed by an ultra-microbalance (Model XP2U, Mettler-Toledo International Inc., Switzerland).

Moreover, due to the reason in above, this study tried to examine the influence of northeast monsoon on Aeolian dust from the riverbed. Thus, the ambient wind speed and direction detector (Weather Wizard III, Davis Instruments, USA) was not only installing on horizontal sampling site but also used to measure the vertical wind situation at 1 meter, 3 and 5 meters heights in the source site sampling.

RESULTS AND DISCUSSION

Aeolian dust from riverbed was an important source to affect the ambient air quality and the human health. The dust suspension from the riverbed was influenced by some properties, such as the bare zone size, moisture content, weather conditions and sediment properties. Therefore, the following section investigated the covering condition of the riverbed, and ambient air quality by the horizontal/ vertical sampling.

Covering and Weather Conditions of Jhuoshuei River

Covering condition of the riverbed was one of the most important properties on dust emission. Fig. 2 showed the downstream covering condition of the Jhuoshuei River on January 5th, 2011 by using the UAV photography system. According to the computational chromatic analysis, the results indicated that the bare zone was about 50.1% of the total riverbed zone. Besides, the effective bare area was smaller due to the land surface crusting or something covering. The partial land of bare area was obviously covered with dry straws by farmers due to the preparation of watermelon planting. Furthermore, as shown in Fig. 2, there were two types of surface crusting, first one was thin slice (< 1 cm), and another was thick cake (about 3 cm in average). Those surface crusts protected the riverbed to reduce the effect of Aeolian process.

Along with Fig. 2, the green covering was about 16.8%. Therefore, the other area could be regarded as the water covering and wetlands near the water, however, the water covering and wetlands were difficult to recognize. Finally, this study changed the contrast and the RGB intensity of the image to discriminate the water zone and wetlands. According to this method, the water covering was about 17.4% and the wetlands was about 15.7% of the total riverbed.

In addition, the weather in the study zone was less rain and almost at dry condition from October 2010 to April 2011. The average value of monthly accumulated precipitation was only around 18.14 mm at these seven months (data from Yun-Lin weather station, Central Weather Bureau, Taiwan). Besides, the precipitous topography procures the short residence time of the river stream in Taiwan. Therefore, in measuring period, the riverbed lied in the semi-dry condition. The Aeolian dust might influence the nearby village ambient air quality severely during the windy weather situation.

Horizontal and Vertical Characteristics of Aeolian Dust

According to the above reason, this study investigated two event cases, the first case happened on November 26th, 2010, and the second case was on January 15th, 2011. The first case was the Aeolian dust emission in slower wind speed condition. Then the dust emission of faster wind speed condition was probed in the other case. The following results were discussing the particulate matter mass distribution and wind profile according to the vertical and horizontal sampling.

(A) First Case (November 26th, 2010)

In principle, the weather condition was an important factor of Aeolian dust suspension and diffusion, and it's also a vital project of ambient air quality. The stronger northeast monsoon happened on November 26th, 2010. The wind direction was almost blowing from the north to the south as shown in Fig. 3. Wind speed is one of the most important factors in dust suspension. The hourly average wind speed was about 2.7 m s^{-1} and the maximum hourly wind speed was about 4.5 m s^{-1} in Lun-Bei air quality monitoring station (from 10 a.m. to 6 p.m.). Nevertheless, the average wind speed in the source site (five meters height, from noon to 5 p.m.) was about 6.03 m s^{-1}, and the maximum wind speed was 8.5 m s^{-1}, as shown in Fig. 3. In fact, the discrepancy of wind speed in the atmospheric boundary-layer was influenced by terrain, vegetation and

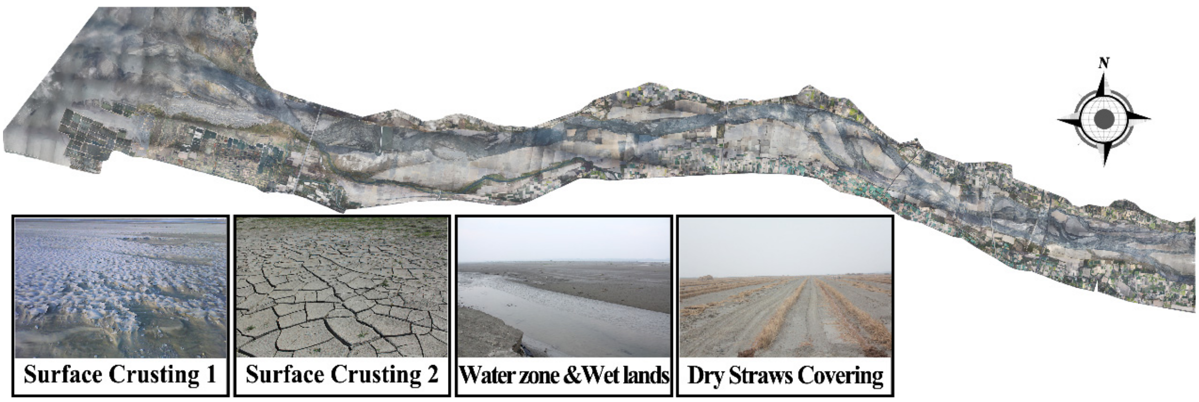

Fig. 2. The unmanned aerial vehicle (UAV) imagery of target arid riverbed, besides, the photos under the UAV imagery shown two types crusting, water zone, wet lands, and dry straws covering on January 5th, 2011.

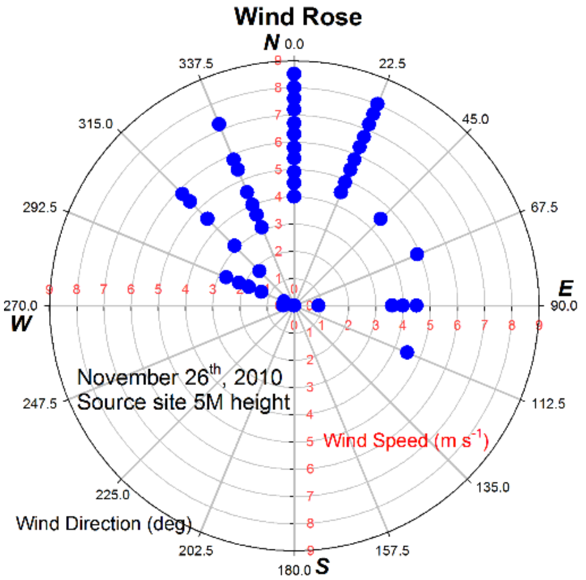

Fig. 3. The wind rose at the source site on November 26th, 2010.

structure (Conan *et al.*, 2015) due to the surface roughness length increasing (Tieleman, 2003). Besides, the accumulated precipitation from November 23th to 26th, 2010 was zero in order to obviate the influences of moisture.

In horizontal sampling, the PM size distribution and mass concentration were measured by using model 298 Marple sampler. As demonstrated in Fig. 4, the PM mass concentration in the source site was larger than other sites. The total mass concentration ratio of south site to source site (1 meter height sampling) was about 1:9. Fig. 4 also indicated that the mode of Aeolian dust in the source site was about 14.8 µm (coarse particle). However, the south site was affected by fine particle. In principle, the obstacle and covering drop the wind speed, therefore, suspension particle retard and deposit easily (Youssef *et al.*, 2012). Especially, the vegetation covered riverbed increase the surface roughness and roughness height (Counihan, 1975; Tieleman, 2003), it change the Aeolian dust diffusion. According to these reasons, at slower wind speed condition, the downstream village's ambient air quality might not be affected by coarse dust even if the sediment suspension from riverbed. However, as the result of exposure risk studies, the particle size of primary pulmonary deposition was below 0.1 µm (Sahu *et al.*, 2013; Patterson *et al.*, 2014). It should pay attention to the effect of Aeolian dust on health even in slower wind speed condition.

Table 1 exposed the vertical sampling data which included PM concentration, size distribution, and wind speed in each sampling height. First, the total PM concentration almost decreased with increasing sampling height. Besides, in this case, the coarse dust was measured at one meter height principally. However, the fine dust almost distributed at two meters height. The results proved that the primary contribution of Aeolian dust was on coarse particle, additionally, the wind blow suspension height of fine particle was greater than coarse size particle. It verified that the coarse particle deposited in the vicinage by gravitational settling and aerodynamic drag force. Moreover, Table 1 revealed wind speed in each sampling height also. According to the equation of wind profile (Eq. (1)), if the Von Kármán constant is about 0.4 (atmospheric condition, Zhang *et al.*, 2008), the calculation surface roughness height and friction velocity was about 3.08 mm and 0.33 m s^{-1}, respectively, in this case. The surface roughness height was almost the same with WMO's report in 2008. In mud flats or snow with no vegetation and obstacle situation, the surface roughness height was about 5 mm (WMO, 2008).

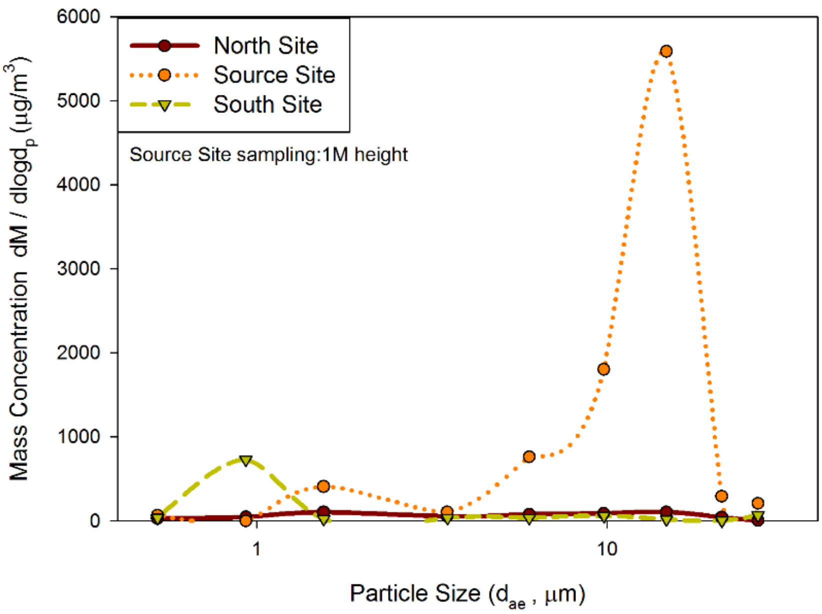

Fig. 4. The PM mass concentration and size distribution of horizontal sampling by using model 298 Marple samplers on November 26th, 2010.

Table 1. The vertical sampling PM properties and wind speeds of "case I" in each sampling height.

Sampling Height	Aerodynamic particle cut-point (d_{50}, μm) of each stages									Wind Speed
	27	*21.3*	*14.8*	*9.8*	*6*	*3.5*	*1.55*	*0.93*	*0.52*	m s^{-1} (Av.)
1 meter	206.8	290.1	**5585.2**	**1801.2**	759.3	103.7	407.4	N.D	66.7	4.72
2 meters	796.3	264.8	59.3	85.2	307.4	407.4	**2470.4**	**3755.6**	418.5	
3 meters	192.6	137	18.5	120.4	251.9	170.4	51.9	48.1	133.3	5.41
4 meters	1307.4	1692.6	177.8	177.8	33.3	403.7	151.9	181.5	259.3	
5 meters	592.6	322.2	192.6	37	111.1	322.2	44.4	59.3	66.7	6.03

a. Marple 298 sampler flow rate is 2 L min^{-1}.
b. Unit of PM concentration is μg m^{-3}.

$$u_z = \frac{u_*}{\kappa}\ln\left(\frac{z}{z_0}\right) \quad (1)$$

where the u_z is the mean wind speed at height z (m) above the ground; κ is the Von Kármán constant; u_* is the friction velocity (m s^{-1}); z_0 is the surface roughness (m).

(B) Second Case (January 15th, 2011)

The weather condition of the second case was also influenced by the northeast monsoon on January 15th, 2011. The cardinal direction of wind was also coming from the north. Besides, rainless condition was also occurred for three days long before sampling, in this case. According to Lun-Bei air quality monitoring station, the hourly average wind speed from 10 a.m. to 6 p.m. was about 8.3 m s^{-1} and the maximum hourly wind speed tended to 11.0 m s^{-1}. In addition, the average wind speed in the source site (five meters height, noon to 3 p.m.) was about 14.0 m s^{-1}, and the maximum wind speed was around 16.9 m s^{-1}, as presented in Fig. 5. The wind speed of this case was higher than the first case undoubtedly.

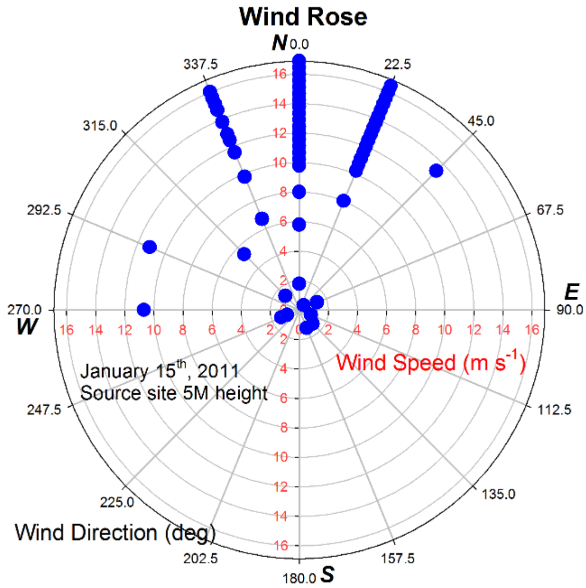

Fig. 5. The wind rose at the source site on January 15th, 2011.

Fig. 6 exhibited that the particulate matter size distribution and mass concentration of horizontal sampling in the second case. PM mass concentration of south site was progressively decreasing in the wake of that the dust cloud was crossing a length of distance, however, it's also higher than the north site. The total mass concentration ratio of south site to source site (1 meter height sampling) was about 1:3. And the particle mass size characteristics of Aeolian dust were distributed in a bimodal or a multimodal curve (Dobrzhinsky *et al.*, 2012). The available evidence giving the same information with other studies, coarse particle with the size greater than 10 μm was the major effect upon source atmospheric or dust cloud, as the windblown dust condition (Neff *et al.*, 2013). Besides, other peaks were below 5 μm particle that was also suspended near ground obviously. However, the majority Aeolian dust size of transmission in the atmosphere was between 0.1 and 10 μm (Maring *et al.*, 2003), due to the differences in the gravitational settling rate of each particle size (Mahowald *et al.*, 2014). The result in this case revealed that the south site was evidently under the influence of Aeolian dust from the riverbed, especially in coarse size particle.

Table 2 exposed the vertical sampling data which included PM concentration, size distribution, and wind speed in each sampling height in this case. It has clearly demonstrated that Aeolian dust total mass concentration was increased, but the particle mass mode size was decreased, as the vertical sampling height increasing except one meter height. Besides, the particle deposition also made the most part of coarse particle remaining in the vicinage of the source. However, the Aeolian dust transportation distance at faster wind speed condition was farther than slower wind speed condition. According to the wind speed data and wind profile equation, the calculation of surface roughness height and friction velocity was about 1.07 mm and 0.68 m s^{-1}, respectively, at faster wind speed situation.

Comparison and Discussion

Comparing with these two cases, Fig. 7 showed the total particle mass concentration of each sampling sites. The tendency of vertical total particle mass concentration displayed the cross curves in the source site. In case I, the total particle mass concentration was decreased as increasing the sampling height due to the less fine particle suspension and the shorter coarse particle deposition distance under the slower wind speed condition. Contrarily, in case II, the total particle mass concentration was increased as increasing the sampling height except one meter height sampling under the faster wind speed condition. Moreover, as the wind speed

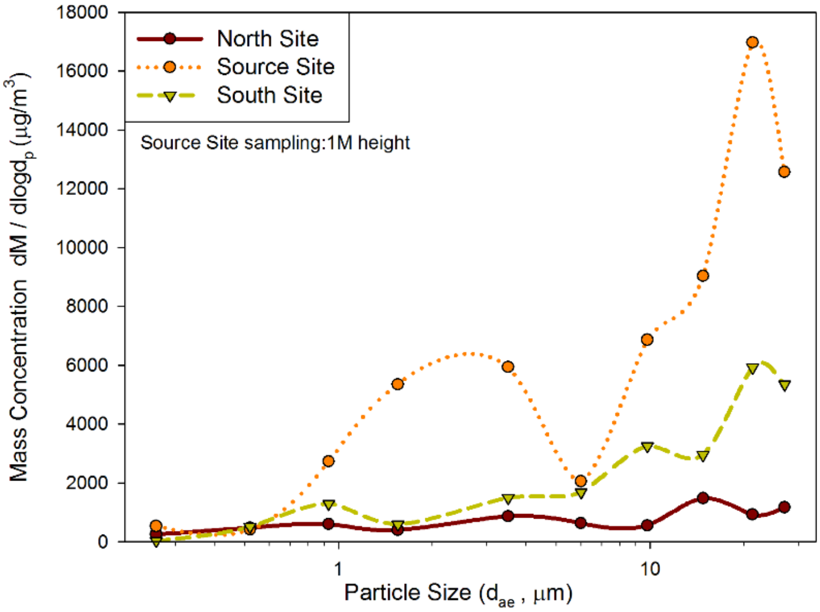

Fig. 6. The PM mass concentration and size distribution of horizontal sampling by using model 298 Marple samplers on January 15th, 2011.

Table 2. The vertical sampling PM properties and wind speeds of "case II" in each sampling height.

Sampling	Aerodynamic particle cut-point (d_{50}, μm) of each stages									Wind Speed
Height	*27*	*21.3*	*14.8*	*9.8*	*6*	*3.5*	*1.55*	*0.93*	*0.52*	m s^{-1} (Av.)
1 meter	**1156.7**	**2145.6**	**1504.4**	**1319.9**	454	**1629.9**	**1651.4**	637.5	1997.3	11.34
2 meters	1140.8	422.5	573.9	707.7	758.8	603.9	493	160.2	1146.1	
3 meters	834.5	697.2	369.7	1158.5	431.3	579.2	304.6	120.6	1795.8	13.16
4 meters	1926.1	568.7	538.7	537	647.9	**1957.7**	206	598.6	1361.8	
5 meters	707.7	**1727.1**	**2073.9**	737.7	899.6	**5207.7**	1031.7	702.5	1466.6	14.04

a. Marple 298 sampler flow rate is 2 L min^{-1}.
b. Unit of PM concentration is μg m^{-3}.

increased, the accumulation concentration of suspension particle was increased. Consistent with Hinds (1999), the faster the wind speed is, the greater the probability of re-entrainment is.

In principle, according to the wind gradient, the parallel wind speeds near the ground approach to zero due to the non-slip condition. And the faster the wind is, the shorter the surface roughness height is (Hartmann, 2015). Due to the faster wind speed situation, the mass concentration of one meter height sampling was almost higher than other sampling heights. Hence, as presented in Table 2, the particle mode size of one meter height sampling was about 21.3 µm (d_{50} by mass). In addition, this phenomenon was also happened under the slower wind speed condition as shown in the Table 1, however, the suspension particle was became smaller (14.8 µm, d_{50} by mass). The results conformed to the physical theory of particle motion near the surface.

The result occurred by two processes, including erosion and denudation, especially in erosion process. Due to the wind active, the sand or gravel motion can make the corrasion and the attrition function. These are important processes of mechanical erosion in the earth's surface which may produce the smaller particulate. Besides, the particle size made the force difference, the larger the particle is, the lower the inter-particle force is (Kok *et al.*, 2012). On the other hand, smaller particle might be hidden by the larger particle at the same flat that obstructed the fine particle resuspension. It was called the shielding effect of particle motion (Agudo *et al.*, 2014; Wang and Arson, 2016). Therefore, the fraction of fine particle suspension was lower than coarse particle during the slower wind speed condition. However, if it's under the high wind force situation, the fine particle could suspend easier. As the most of health risk studies, the influence of fine Aeolian dust should be paid more attention (Kavouras *et al.*, 2015; He *et al.*, 2016).

CONCLUSIONS

The Aeolian dust from the semi-arid riverbed of Jhuoshuei River is an important PM emission source in Taiwan. According to the UAV photography and computational chromatic analysis, the percentage of riverbed covering conditions, including bare zone, wetlands, green covering and water covering was 50.1, 15.7, 16.8 and 17.4%, respectively, in January 5th, 2011. However, in bare zone, partial land was covered with dry straws or dry sediment crust. The result

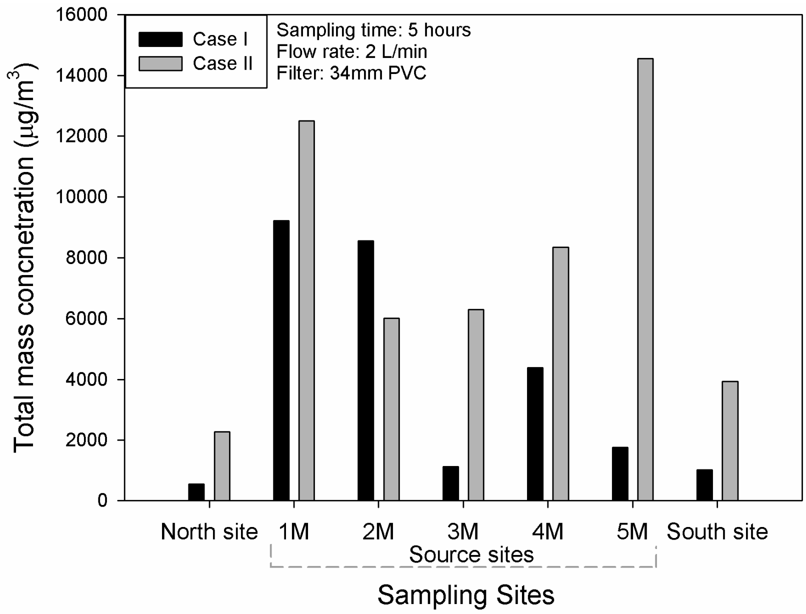

Fig. 7. The total PM mass concentration of two cases sampling by using model 298 Marple samplers.

indicated that the dust emission rate might be different with fully bare condition. Nonetheless, the Aeolian dust might influence the nearby village ambient air quality severely due to the rainless and northeast monsoon weather condition.

Therefore, two different wind speed conditions were investigated and discussed in this study, the first case happened in November 26th, 2010, and the second case was on January 15th, 2011. The influence factor of downstream village's ambient air quality on river dust was the wind speed and distance between source and receptor. According to the horizontal results, the total mass concentration ratio of south site to source site (one meter height) was about 1:9 in first case and about 1:3 in second case. The ratio shown the influence index of Aeolian dust. The receptor was evidently under the influence of Aeolian dust from the riverbed, especially in coarse size particle in the second case. Moreover, the particle mass size characteristics of Aeolian dust were distributed in a bimodal or a multimodal curve, and the main peak size was above 10 μm. As the force balance between gravity settling and wind blowing of particle, the particle mode size (one meter height sampling) of faster wind speed case (about 21.3 μm, d_{50} by mass) was larger than slower wind speed case (about 14.8 μm, d_{50} by mass). Besides, in the first case, the total PM concentration was almost decreased with increasing sampling height, however, the second case was just the reverse. Shielding effect of particle motion made that the suspension of fine particle was more difficult than coarse particle during the slower wind speed condition.

According to the wind profile, the calculation surface roughness height of the case I and case II was about 3.08 mm and 1.07 mm, respectively, and the friction velocity was about 0.33 m s^{-1} and 0.68 m s^{-1}, respectively. Comparing with those two cases, the faster the wind is, the shorter the surface roughness height is. Owing to the above reason and the comparative result of those two cases, the faster wind speed caused the greater fine particle suspension and the higher suspension height.

Aeolian dust is an important issue, where covered not only in local but also in global. Besides, the phenomena of Aeolian dust combine lots of complicated processes. Consequently, this study clued the spatial variability of river dust events, which can further aid the site investigating, forecasting and preventing of dust influence.

ACKNOWLEDGMENTS

The data in this field study were all collected and analyzed by the authors. All authors extremely thank for the generosity support from Environmental Protection Administration and Ministry of Science and Technology, Taiwan (grant numbers NSC 99-EPA-M-008-001). Besides, we also thank the support from Central Weather Bureau, which maintains the weather monitoring and helps us to judge whether go for sampling or not. The present study would not have been completed without the support of those departments.

REFERENCES

Agudo, J.R., Dasilva, S. and Wierschem, A. (2014). How do neighbors affect incipient particle motion in laminar shear flow? *Phys. Fluids* 26: 053303.

Bagnold, R.A. (1941). *The Physics of Blown Sand and Desert Dunes*, Methuen, London. ISBN: 9780486439310, 265p.

Bauer, E. and Ganopolski, A. (2010). Aeolian dust modeling over the past four glacial cycles with CLIMBER-2. *Global Planet. Change* 74: 49–60.

Bian, H., Tie, X.X., Cao, J.J., Ying, Z.M., Han, S.Q. and Xue, Y. (2011). Analysis of a severe dust storm event over China: Application of the WRF-Dust model. *Aerosol Air Qual. Res.* 11: 419–428.

Chang, C.T. (2006). Characteristics and emission factors of fugitive dust at gravel processing sites. *Aerosol Air Qual. Res.* 6: 15–29.

Chen, X.Y., Spooner, N.A., Olley, J.M. and Questiaux, D.G. (2002). Addition of aeolian dusts to soils in southeastern Australia: Red silty clay trapped in dunes bordering Murrumbidgee River in the Wagga Wagga region. *Catena* 47: 1–27.

Chen, Y.C., Hsu, C.Y., Lin, S.L., Chang-Chien, G.P., Chen, M.J., Fang, G.C. and Chiang, H.C. (2015). Characteristics of concentrations and metal compositions for $PM_{2.5}$ and $PM_{2.5–10}$ in Yunlin County, Taiwan during air quality deterioration. *Aerosol Air Qual. Res.* 15: 2571–2583.

Cheng, Y.C., Liang, C.S., Syu, J.Y., Chang, Y.Y., Yan, Y.L., Chen, S.J., Chen, C.C. and Lin, W.Y. (2015). Characteristics of aerosol extinction coefficient in Taipei metropolitan atmosphere. *Aerosol Air Qual. Res.* 15: 1823–1835.

Conan, B., Aubrun, S., Coudour, B., Chetehouna, K. and Garo, J.P. (2015). Contribution of coherent structures to momentum and concentration fluxes over a flat vegetation canopy modelled in a wind tunnel. *Atmos. Environ.* 107: 329–341.

Counihan, J. (1975). Adiabatic atmospheric boundary layers: A review and analysis of data from the period 1880-1972. *Atmos. Environ.* 9: 871–905.

De, U.S., Dube, R.K. and Rao, G.S.P. (2005). Extreme weather events over India in the last 100 years. *J. Indian Geophys. Union* 9: 173–187.

Delmas, V., Jones, H.G., Tranter, M. and Delmas, R. (1996). The weathering of aeolian dusts in alpine snows. *Atmos. Environ.* 30: 1317–1325.

Dobrzhinsky, N., Krugly, E., Kliucininkas, L., Prasauskas, T., Kireitseu, M., Zerrath, A. and Martuzevicius, D. (2012). Characterization of desert road dust aerosol from provinces of Afghanistan and Iraq. *Aerosol Air Qual. Res.* 12: 1209–1216.

Erell, E. and Tsoar, H. (1999). Spatial variations in the aeolian deposition of dust– the effect of a city: A case study in Be'er-Sheva, Israel. *Atmos. Environ.* 33: 4049–4055.

Evan, A.T., Flamant, C., Fiedler, S. and Doherty, O. (2014). An analysis of aeolian dust in climate models. *Geophys. Res. Lett.* 41: 5996–6001.

Fang, G.C., Lin, S.J., Chang, S.Y. and Chou, C.C.K. (2009). Effect of typhoon on atmospheric particulates in autumn in central Taiwan. *Atmos. Environ.* 43: 6039–6048.

Field, J.P., Breshears, D.D. and Whicker, J.J. (2009). Toward a more holistic perspective of soil erosion: Why aeolian research needs to explicitly consider fluvial processes and interactions. *Aeolian Res.* 1: 9–17.

Field, J.P., Breshears, D.D., Whicker, J.J. and Zou, C.B. (2012). Sediment capture by vegetation patches: Implicationsfor desertification and increased resource redistribution. *J. Geophys. Res.* 117: G01033.

Friedlander, S.K. (2000), *Smoke, Dust, and Haze: Fundamentals of Aerosol Dynamics*, Oxford University Press, Oxford. ISBN: 9780195129991.

Furieri, B., Russeil, S., Santos, J.M. and Harion, J.L. (2013). Effects of non-erodible particles on aeolian erosion: Wind-tunnel simulations of a sand oblong storage pile. *Atmos. Environ.* 79: 672–680.

Ghim, Y.S., Chang, Y.S. and Jung K. (2015). Temporal and spatial variations in fine and coarse particles in Seoul, Korea. *Aerosol Air Qual. Res.* 15: 842–852.

Goossens, D. and Offer, Z.Y. (1997). Aeolian dust erosion on different types of hills in a rocky desert- wind tunnel simulations and field measurements. *J. Arid. Environ.* 37: 209–229.

Goossens, D. and Offer, Z.Y. (2000). Wind tunnel and field calibration of six aeolian dust samplers. *Atmos. Environ.* 34: 1043–1057.

Goudie, A.S. (2009). Dust storms: Recent developments. *J. Environ. Manage.* 90: 89–94.

Goudie, A.S. (2014). Desert dust and human health disorders. *Environ. Int.* 63: 101–113.

Greeley, R., White, B.R., Pollack, J.B., Iversen, J.D. and Leach, R.N. (1977). Dust storms on mars: Considerations and simulations. *NASA Technical Memorandum*, 78423.

Hahnenberger, M. and Nicoll, K. (2012). Meteorological characteristics of dust storm events in the eastern Great Basin of Utah, U.S.A. *Atmos. Environ.* 60: 601–612.

Hahnenberger, M. and Nicoll, K. (2014). Geomorphic and land cover identification of dust sources in the eastern Great Basin of Utah, U.S.A. *Geomorphology* 204: 657–672.

Hartmann, D.L. (2015). Chapter 4: The Energe Balance of the Surface. In *Global physical climatology (2nd ed.)*, Academic Press, California, pp. 95–129.

He, M., Ichinose, T., Kobayashi, M., Arashidani, K., Yoshida, S., Nishikawa, M., Takano, H., Sun, G. and Shibamoto, T. (2016). Differences in allergic inflammatory responses between urban $PM_{2.5}$ and fine particle derived from desert-dust in murine lungs. *Toxicol. Appl. Pharmacol.* 297: 41–55.

Hinds, W.C. (2000). *Aerosol Technology: Properties, Behavior, and Measurement of Airborne Particles*, John Wiley and Sons, New York. ISBN: 9781118591567, 464 p.

Hugenholtz, C.H., Levin, N., Barchyn, T.E. and Baddock, M.C. (2012). Remote sensing and spatial analysis of aeolian sand dunes: A review and outlook. *Earth Sci. Rev.* 111: 319–334.

In, H.J. and Park, S.U. (2003). The soil particle size dependent emission parameterization for an Asian dust (Yellow Sand) observed in Korea in April 2002. *Atmos. Environ.* 37: 4625–4636.

Karanasiou, A., Amato, F., Moreno, T., Lumbreras, J., Borge, R., Linares, C., Boldo, E., Alastuey, A. and Querol, X. (2014). Road dust emission sources and assessment of street washing effect. *Aerosol Air Qual. Res.* 14: 734–743.

Kavouras, I.G., DuBois, D.W., Nikolich, G. and Etyemezian, V. (2015). Monitoring, source identification and health risks of air toxics in Albuquerque, New Mexico, U.S.A. *Aerosol Air Qual. Res.* 15: 556–571.

Kim, J.Y., Yoon, S.C., Jefferson, A. and Kim, S.W.

(2006). Aerosol hygroscopic properties during Asian dust, pollution, and biomass burning episodes at Gosan, Korea in April 2001. *Atmos. Environ.* 40:1550–1560.

King, J., Etyemezian, V., Sweeney, M., Buck, B.J. and Nikolich, G. (2011). Dust emission variability at the Salton Sea, California, USA. *Aeolian Res.* 3: 67–79.

Kok, J.F. (2012). Does the size distribution of mineral dust aerosols depend on the wind speed at emission? *Atmos. Chem. Phys*. 11: 10149–10156.

Kok, J.F., Parteli, E.J.R., Michaels, T.I. and Bou Karam, D. (2012). The physics of wind-blown sand and dust. *Rep. Prog. Phys.* 75: 106901.

Lancaster, N. (2013). 13.9 Climate Change and Aeolian Processes. In *Treatise on Geomorphology*, Vol. 13, Geomorphology of Human Disturbances, Climate Change, and Natural Hazards, Academic Press, San Diego, pp. 132–151.

Lequy, É., Conil, S. and Turpault, M.P. (2012). Impacts of aeolian dust deposition on European forest sustainability: A review. *For. Ecol. Manage.* 267: 240–252.

Li, C.S., Shi, X.F., Kao, S.J., Liu, Y.G., Lyu, H.H., Zou, J.J., Liu, S.F. and Qiao, S.Q. (2013). Rare earth elements in fine-grained sediments of major rivers from the high-standing island of Taiwan. *J. Asian Earth Sci.* 69: 39–47.

Liang, C.S., Yu, T.Y. and Lin W.Y. (2015). Source apportionment of submicron particle size distribution and $PM_{2.5}$ composition during an Asian dust storm period in two urban atmospheres. *Aerosol Air Qual. Res.* 15: 2609–2624.

Lin, C.W. and Yeh, J.F. (2007). Estimating dust emission from a sandbank on the downstream Jhuoshuei River under strong wind conditions. *Atmos. Environ.* 41: 7553–7561.

Mahowald, N., Albani, S., Kok, J.F., Engelstaeder, S., Scanza, R., Ward, D.S. and Flanner, M.G. (2014). The size distribution of desert dust aerosols and its impact on the earth system. *Aeolian Res.* 15: 53–71.

Margielewski, W., Krąpiec, M., Jankowski, L., Urban, J. and Zernitskaya, V. (2015). Impact of aeolian processes on peat accumulation: Late Glacial–Holocene history of the Hamernia peat bog (Roztocze region, south-eastern Poland). *Quat. Int.* 386: 212–225.

Maring, H., Savoie, D.L., Izaguirre, M.A., Custals, L. and Reid, J.S. (2003). Mineral dust aerosol size distribution change during atmospheric transport. *J. Geophys. Res.* 108: 8592.

McGowan, H.A., Sturman, A.P. and Owens, I.F. (1996). Aeolian dust transport and deposition by foehn winds in an alpine environment, Lake Tekapo, New Zealand. *Geomorphology* 15: 135–146.

Modaihsh, A.S. and Mahjoub, M.O. (2013). Falling dust characteristics in Riyadh city, Saudi Arabia during winter months. *APCBEE Procedia* 5: 50–58.

Moridnejad, A., Karimic, N. and Ariya, P.A. (2015). Newly desertified regions in Iraq and its surrounding areas: Significant novel sources of global dust particles. *J. Arid. Environ.* 116: 1–10.

Neff, J.C., Reynolds, R.L., Munson, S.M., Fernandez, D. and Belnap, J. (2013). The role of dust storms in total atmospheric particle concentrations at two sites in the western U.S. *J. Geophys. Res.* 118: 11201–11212.

Offer, Z.Y. and Goossens, D. (1995). Wind tunnel experiments and field measurements of aeolian dust deposition on conical hills. *Geomorphology* 14: 43–56.

Ono, D. (2006). Application of the Gillette model for windblown dust at Owens Lake, CA. *Atmos. Environ.* 40: 3011–3021.

Patterson, R.F., Zhang, Q., Zheng, M. and Zhu, Y. (2014). Particle deposition in respiratory tracts of school-aged children. *Aerosol Air Qual. Res.* 14: 64–73.

Pillai, P.S., Babu, S.S. and Moorthy, K.K. (2002). A study of PM, PM_{10} and $PM_{2.5}$ concentration at a tropical coastal station. *Atmos. Res.* 61: 149–167.

Pokhrel, R.J. and Lee, H.W. (2011). Estimation of the effective zone of sea/land breeze in a coastal area. *Atmos. Pollut. Res*. 2: 106–115.

Pui, D.Y.H., Chen, S.C. and Zuo, Z. (2014). $PM_{2.5}$ in China: Measurements, sources, visibility and health effects, and mitigation. *Particuology* 13: 1–26.

Rashki, A., Eriksson, P.G., de Rautenbach, C.J.W., Kaskaoutis, D.G., Grote, W. and Dykstra, J. (2013). Assessment of chemical and mineralogical characteristics of airborne dust in the Sistan region, Iran. *Chemosphere* 90: 227–236.

Reynolds, R.L., Reheis, M., Yount, J. and Lamothe, P. (2006). Composition of aeolian dust in natural traps on isolated surfaces of the central Mojave Desert- Insights to mixing, sources, and nutrient inputs. *J. Arid. Environ*. 66: 42–61.

Saffman, P.G. (1965). The lift on a small sphere in a slow shear flow. *J. Fluid Mech*. 22: 385–400.

Sahu, S.K., Tiwari, M., Bhangare, R.C. and Pandit G.G. (2013). Particle size distribution of mainstream and exhaled cigarette smoke and predictive deposition in human respiratory tract. *Aerosol Air Qual. Res.* 13: 324–332.

Sharratt, B.S. and Vaddella, V. (2014). Threshold friction velocity of crusted windblown soils in the Columbia Plateau. *Aeolian Res.* 15: 227–234.

Shen, K.J., Li, W.F., Pei, Z.Y., Fei, W., Sun, G.N., Zhang, X.Q., Chen, X.W. and Ma, S.J. (2015). Crop area estimation from UAV transect and MSR image data using spatial sampling method. *Procedia Environ. Sci.* 26: 95–100.

Siame, L.L., Angelier, J., Chen, R.F., Godard, V., Derrieux, F., Bourlès, D.L., Braucher, R., Chang, K.J., Chu, H.T. and Lee, J.C. (2010). Erosion rates in an active orogen (NE-Taiwan): A confrontation of cosmogenic measurements with river suspended loads. *Quat. Geochronol.* 6: 246–260.

Tieleman, H.W. (2003). Roughness estimation for wind-load simulation experiments. *J. Wind Eng. Ind. Aerodyn.* 91: 1163–1173.

Upadhyay N., Clements, A.L., Fraser, M.P., Sundblom, M., Solomon, P. and Herckes, P. (2015). Size-differentiated chemical composition of re-suspended soil dust from the desert southwest United States. *Aerosol Air Qual. Res.* 15: 387–398.

Vickery, K.J. and Eckardt, F.D. (2013). Dust emission controls on the lower Kuiseb River valley, Central Namib. *Aeolian Res.* 10: 125–133.
Vijayakumar, K., Devara, P.C.S., Raoa, S.V.B. and Jayasankar, C.K. (2016). Dust aerosol characterization and transport features based on combined ground-based, satellite and model-simulated data. *Aeolian Res.* 21: 75–85.
Wang, P. and Arson, C. (2016). Discrete element modeling of shielding and size effects during single particle crushing. *Comput. Geotech.* 78: 227–236.
Webb, N.P. and Strong, C.L. (2011). Soil erodibility dynamics and its representation for wind erosion and dust emission models. *Aeolian Res*. 3: 165–179.
WMO (2008). Annex: The Effective Roughness Length. Guide to Meteorological Instruments and Methods of Observation (7th ed.), World Meteorological Organization, Geneva, pp. I.5–12. ISBN 978-92-63-10008-5
Yang, M.D., Lin, J.Y., Yao, C.Y., Chen, J.Y., Su, T.C. and Jan, C.D. (2011). Landslide-induced levee failure by high concentrated sediment flow - A case of Shan-An levee at Chenyulan River, Taiwan. *Eng. Geol.* 123: 91–99.
Youssef, F., Visser, S.M., Karssenberg, D., Erpul, G., Cornelis, W.M., Gabriels, D. and Poortinga, A. (2012). The effect of vegetation patterns on wind-blown mass transport at the regional scale: A wind tunnel experiment. *Geomorphology* 159–160: 178–188.
Zhang, Y., Ma, J. and Cao, Z. (2008). The Von Kármán constant retrieved from CASES-97 dataset using a variational method. *Atmos. Chem. Phys.* 8: 7045–7053.
Zhao, X.P. (2012). Asian dust detection from the satellite observations of moderate resolution imaging spectroradiometer (MODIS). *Aerosol Air Qual. Res.* 12: 1073–1080.
Zhu, B.Q. and Yu, J.J. (2014). Aeolian sorting processes in the Ejina desert basin (China) and their response to depositional environment. *Aeolian Res.* 12: 111–120.

Received for review, August 9, 2016
Revised, October 1, 2016
Accepted, October 2, 2016